Thesis Summary

Wave Interaction with Underground Openings in Fractured Rock

by Mark William Hildyard

Abstract

This thesis aims to develop improved models of seismic wave propagation around underground openings by modelling the interaction of waves with the fractured rock surrounding these openings. Its primary motivation comes from the needs of industries which have stability problems, such as deep-level mining which has the rockburst problem, or nuclear waste storage where extremely long-term stability is required. Deficiencies are identified in previous modelling. Few attempts have been made to compare the simulated waves with observed seismic waves, and where this has been attempted, the correspondence of waveforms near the surface of an excavation has been poor. The thesis applies models to observations from controlled experiments and demonstrates that wave propagation can be reliably and accurately modelled. In so doing it motivates its application to the larger problem.

A three-dimensional finite difference model is used to simulate wave behaviour. The thesis covers the theory of its staggered-grid scheme and the implementation of fractures and cavities. A practical method is developed to calculate numerical dispersion. Applying this to a number of different codes, indicates that general-purpose codes can be up to two orders of magnitude less efficient at wave propagation problems, which severely limits the size of problem to which they can be applied. The scheme used is efficient but limited to orthogonal geometries. Methods are investigated which allow generalisation of this scheme without loss of efficiency. A new grid scheme, which has the same order of accuracy and efficiency as the staggered grid, is proposed for future development.

Laboratory experiments, which passed seismic waves through multiple plates representing aligned fractures, are modelled numerically using multiple displacement discontinuities. There is a striking correspondence between the simulated and observed waveforms and the effect of the fractures on wave-speed and attenuation. However, a significant discrepancy is evident in the numerical waveforms for wave propagation across fractures. The model is modified to include the effects of a non-uniform stress state using stress dependent fracture stiffness. The wave-fracture modelling is extended to *in situ* fractures in rock at the surface of a deep tunnel, using data collected in an acoustic emission experiment at the URL Mine-by tunnel. Waveforms from the velocity scans are compared against those from elastic models and various models of fracture, such as random assemblies of small open cracks and larger fractures with a fracture stiffness. A generic method is also developed for calculating the frequency variation of wave-speed and amplitude for collections of cracks. Results indicate that it is possible to account for the wave-speeds and amplitudes using models with fractures. The models of fracture are then applied to the rockburst problem to investigate the effect of an excavation on the amplitude and the distribution of ground motion. This provides important insights into the causes of effects such as the apparent amplification observed by researchers in this field.

1. Introduction

This thesis seeks to evaluate and improve models of wave propagation around underground openings in fractured rock. Its motivation is two-fold. The first application is for addressing the rockburst problem in deep-level mining. One approach being pursued is to develop numerical models of rockbursts which project the amplitudes and distribution of seismic wave motion around an excavation. Since the rock surrounding such excavations is fractured, this requires the development of models of wave propagation through fractures. The second application is to increase understanding of what the seismic waves indicate about the state of fracturing. This is very important not only in the mining industry but in other industries including oil extraction and nuclear waste storage.

The thesis introduces the rockburst problem, and issues which are poorly understood, such as high ground velocities (e.g. McGarr, 1993; Spottiswoode et al., 1997) and the distribution of damage (Durrheim et al., 1997). Simulation of such events could provide important feedback into the safety design process including assessment of regions of likely damage and support requirements. A review of previous applications of wave propagation models to the rockburst problem highlights limitations. There is a need for three-dimensional simulation and a need for evidence of reliable simulation through comparison with observed seismograms. In particular, models need to prove capable of accurately representing wave propagation in the excavation's fracture zone.

The interaction of waves with fracturing has been identified as crucial by prominent researchers in the field of rock mechanics (e.g. Cook, 1992). Much research has been conducted, with significant experimental achievements and greater understanding of the physics. A displacement discontinuity has been proposed as a suitable discrete representation of a fracture (Schoenberg, 1980; Myer et al., 1985). Experimental studies indicate that this representation captures many of the frequency-dependent effects on waves due to fracturing (Pyrak-Nolte, 1990a, 1990b). An alternative approach attempts to encapsulate the effects of large numbers of fractures into the behaviour of the medium. The fractured rock is then treated as an effective elastic medium, with the elastic constants related to the density of fracturing, typically leading to anisotropy in the seismic velocities (e.g. O' Connell and Budiansky, 1974; Crampin, 1981; Sayers and Kachanov, 1991). Expressions for the effective attenuation have also been developed (Hudson, 1981; Liu et al., 2000).

However, a review shows that most numerical studies of waves through fractures make some of the following assumptions: two-dimensional wave-propagation; plane wave propagation; small amplitude motions; low frequencies relative to the crack-size; dilute crack concentration; uniform stress state, or are only accurate for first arrivals. Many of these assumptions are poor in the context of real problems.

Wave motion is non-planar and three-dimensional analysis is essential. Excavations are in a highly non-uniform stress-field and in the case of deep-level mining, the excavation surface is highly fractured, wave amplitudes may be large, and sources are in the near-field. Microseismic and ultrasonic recordings contain frequencies which do not satisfy low frequency and plane wave assumptions, while accurate simulation is required over the full duration of dynamic motion and not just first arrivals, so that the full effect on the rockmass can be assessed.

There is therefore a significant gap between numerical studies to date and what is required for models of wave propagation around underground excavations. It remains to be demonstrated through comparison of simulations with observed behaviour, that such models are capable, appropriate and accurate for simulating wave motion in the zone of fractured rock surrounding a typical underground excavation. This thesis aims to redress these deficiencies. The objectives are:

- Develop numerical models capable of studying wave propagation around underground openings and through fractures.
- Evaluate the capacity to simulate wave propagation through large numbers of fractures by directly comparing simulations with experimental and *in situ* data.
- Demonstrate the contribution that these models can make in applied research, such as in understanding the distribution of ground motion due to underground seismic events, and aiding interpretation of the fracture state from observed waveforms.

The first chapter introduces these themes, reviews previous work and identifies the objectives. Chapter 2 introduces the numerical basis for the work, describing the method and a number of novel developments. Chapter 3 evaluates the displacement discontinuity model of a fracture by numerically simulating a laboratory experiment with wave propagation through multiple fractures. Chapter 4 extends this modelling to rock at the surface of a deep excavation with an unknown distribution of fractures, using data recorded in underground velocity surveys. Chapter 5 applies these techniques to the rockburst problem, studying how the excavation and fracturing influence the amplitude and distribution of ground motion. Chapter 6 summarises the findings and how they contribute to the fields of numerical methods, understanding wave propagation through fractures, and the applications of projecting wave motions around openings and interpreting fracturing from recorded motions.

2. Theoretical and Numerical Basis for Models

The program WAVE was used throughout this thesis to model seismic wave propagation and interaction with cavities and fractures. This chapter gives a detailed review of the basic concepts such as the mesh scheme and the implementation of a discontinuity used to represent free surfaces and

fractures (Cundall, 1992), and additional developments, such as higher order grid schemes and fracture intersection (Hildyard, 1995). A number of new developments are presented. These focus on how the work in the thesis could be applied to general orientations of fracturing, and include:

- Practical methods for analysing the dispersion accuracy of numerical schemes.
- An efficient scheme for obtaining coupled static and dynamic solutions.
- Three different methods which allow of general orientations of cracks and cavities within the staggered grid scheme.
- An examination of the memory and run-time efficiency of some alternatives to the staggered grid using the above methods for establishing dispersion accuracy.
- New finite difference schemes with comparable efficiency to the 4^{th} order staggered grid scheme.

The chapter first presents the theory on which WAVE is based. The program solves the system of first order wave equations using finite differences on a staggered grid, a method which has been widely used in seismological applications (Madariaga, 1976; Aki and Richards, 1980; Virieux,1984; Graves, 1996). In this formulation, a continuum is discretized into a grid or mesh, with different grid variables computed at different positions in space. Fundamental to the program, and to the thesis, is a zero-width discontinuity in the mesh which can be used to model fractures and openings (Cundall, 1992). This consists of two coincident surfaces on which certain grid variables are continuous while others are discontinuous with separate values for the upper and lower surfaces. The fracture surfaces are coupled by a normal and shear fracture stiffness. The thesis describes the staggered grid method in detail, derives the mesh equations, introduces the problem of numerical dispersion and fourth and higher order approximations. It describes the implementation of fractures as a zero-width displacement discontinuity, frictional slip, crack opening-closing behaviour, crack intersections and cavities, and covers the boundary conditions used to reduce reflections and to solve for static stress states.

Two practical approaches were developed for analysing dispersion in numerical schemes. The methods have an advantage over traditional analytical analyses, as they allow the dispersion of a numerical scheme to be evaluated without requiring knowledge of its solution method and can also be used to analyse complex, non-uniform meshes. Numerical dispersion is an important problem with element and grid-based solutions to the wave equation, where the numerical wave-speed deviates from the elastic wave-speed for high frequencies. The first method involves passing a plane wave through the numerical mesh and recording spatial waveforms at two different times, while the second method requires recording time waveforms at two different positions along the wave path. Taking Fourier transforms of these waveforms and denoting A_1 and A_2 as the amplitude and ϕ_1 and ϕ_2 as the phase functions of these transforms, expressions were obtained for phase velocity as a function of wave-number or frequency. For example, Equation (1) is the relationship for two spatial waveforms.

$$c(\gamma) = \frac{1}{\gamma(t_2 - t_1)}\left[-(\phi_2 - \phi_1) + iLn\left(\frac{A_2}{A_1}\right)\right] \qquad (1)$$

Methods were investigated for generalising the staggered grid scheme to allow for angled cracks. A second order approximation was developed for an explicit angled crack based on the approach of grid-aligned cracks. This implementation is efficient for studying limited orientations of fracturing, but is not suited for modelling general fracture geometries, and its accuracy was not formally evaluated. An approach proposed by Coates and Schoenberg (1995), using a localised distribution of transversely isotropic material to represent fractures, was also implemented, but was shown to give severely inaccurate results for angled fractures with a low fracture stiffness. A third method was to extend an approach by Hestholm and Ruud (1994), who implemented a curved free surface topography by mapping the wave equations and boundary conditions from a curvilinear mesh to a rectangular mesh. The approach was followed to derive equations for a general curved fracture, but it was noted that the implementation on a staggered grid has implications for accuracy, as certain derivatives are not readily approximated.

Alternative finite difference and finite element schemes exist which more readily allow angled fractures. Three general-purpose codes commonly used in rock mechanics were analysed to determine their accuracy and efficiency of wave propagation. The codes studied were UDEC (Itasca, 1993a), FLAC (Itasca, 1993b) and ELFEN (Rockfield, 1999). Efficiency was determined based on the memory and run-times required to obtain the equivalent dispersion accuracy. For two-dimensions, the general-purpose codes were found to be nearly two orders of magnitude less efficient than a fourth order, regular spaced, staggered grid, in both memory requirements and run-time. These general-purpose codes would not support a sufficient number of elements to solve many of the problems dealt with in this thesis and more efficient schemes need to be developed.

Novel finite-difference grid schemes were derived in an attempt to develop an efficient alternative to the fourth order staggered mesh. A family of schemes was investigated based on a four-noded quadrilateral element. A four-noded finite-difference scheme can be formulated in a similar manner to that of the staggered mesh and is readily given fourth order accuracy. This is the same scheme proposed recently by Jianfeng (1997), but unfortunately suffers from a problem termed hour-glassing (Marti and Cundall, 1982; Molenkamp et al., 1992). The program FLAC (Itasca, 1993b) uses a scheme based on quadrilateral elements. It overcomes the problem of hour-glassing by subdividing the quadrilaterals into two overlayed sets of triangles, and using mixed discretization (Marti and Cundall, 1982), where a different discretization is used for the isotropic and the deviatoric components of stress and strain. The approach is inefficient in both memory and run-time, and is only second order accurate

which is inefficient for wave propagation problems. It was shown that this scheme can be reduced to an equivalent but significantly more memory efficient second order velocity-displacement scheme. It was then found that for constant-sized elements, the mixed-discretization scheme can be reformulated into a scheme more similar to the staggered grid scheme, by the addition of two new grid variables (termed σ_a and σ_b). The scheme is illustrated in Figure 1. The scheme was extended to form higher order finite difference schemes, with comparable memory and run-time efficiency to that of the higher order staggered mesh. Compared to the staggered mesh though, it holds the different components of stress at the same point in space, giving it advantages for more general studies of fractures.

$$\dot{\sigma}_{11} = E1\frac{1}{2h}\begin{bmatrix}-1 & 1\\ -1 & 1\end{bmatrix}\dot{u}_1 + E2\frac{1}{2h}\begin{bmatrix}1 & 1\\ -1 & -1\end{bmatrix}\dot{u}_2 \qquad \text{(a)}$$

$$\dot{\sigma}_{22} = E2\frac{1}{2h}\begin{bmatrix}-1 & 1\\ -1 & 1\end{bmatrix}\dot{u}_1 + E1\frac{1}{2h}\begin{bmatrix}1 & 1\\ -1 & -1\end{bmatrix}\dot{u}_2 \qquad \text{(b)}$$

$$\dot{\sigma}_{12} = G\frac{1}{2h}\begin{bmatrix}1 & 1\\ -1 & -1\end{bmatrix}\dot{u}_1 + G\frac{1}{2h}\begin{bmatrix}-1 & 1\\ -1 & 1\end{bmatrix}\dot{u}_2 \qquad \text{(c)}$$

$$\sigma_a = 2G\frac{1}{2h}\begin{bmatrix}1 & -1\\ -1 & 1\end{bmatrix}\dot{u}_1 \qquad \text{(d)} \qquad \sigma_b = 2G\frac{1}{2h}\begin{bmatrix}1 & -1\\ -1 & 1\end{bmatrix}\dot{u}_2 \qquad \text{(e)}$$

$$\ddot{u}_1 = \frac{1}{\rho}\frac{1}{2h}\begin{bmatrix}-1 & 1\\ -1 & 1\end{bmatrix}\sigma_{11} + \frac{1}{\rho}\frac{1}{2h}\begin{bmatrix}1 & 1\\ -1 & -1\end{bmatrix}\sigma_{12} + \frac{1}{\rho}\frac{1}{2h}\begin{bmatrix}-1 & 1\\ 1 & -1\end{bmatrix}\sigma_a \qquad \text{(f)}$$

$$\ddot{u}_2 = \frac{1}{\rho}\frac{1}{2h}\begin{bmatrix}-1 & 1\\ -1 & 1\end{bmatrix}\sigma_{12} + \frac{1}{\rho}\frac{1}{2h}\begin{bmatrix}1 & 1\\ -1 & -1\end{bmatrix}\sigma_{22} + \frac{1}{2h}\begin{bmatrix}-1 & 1\\ 1 & -1\end{bmatrix}\sigma_b \qquad \text{(g)}$$

Figure 1 Velocity-stress finite difference scheme for uniform elements, based on FLAC mixed discretization.

3. Modelling seismic wave propagation through fractures – Laboratory Experiments

A displacement discontinuity has been widely used as an explicit model of a fracture. This chapter investigates the capability to numerically model wave propagation through fractures using displacement discontinuities. Numerical models of discrete fractures are compared with waveforms recorded in experiments passing seismic waves through multiple aligned fractures. A striking

similarity is observed between the numerical and recorded waveforms. However, significant departure of the numerical from the experimental results is noted for wave propagation across fractures. It is shown that a modification to this model may account for these differences, without the need for a fundamentally different model.

As noted in the introduction, two approaches have been pursued for representing seismic wave interaction with fractured rock, either encapsulating the behaviour of fractured rock through an effective elastic medium, or modelling fractures or groups of fractures explicitly. A displacement discontinuity is an explicit model, where the displacements on two surfaces of a zero-thickness interface are discontinuous, and the discontinuity in displacement is coupled to the surface stresses by a fracture stiffness. This fracture stiffness accounts for the existence of asperities and voids between the surfaces of natural fractures. A displacement discontinuity is widely used in rock mechanics for studying static behaviour. In these cases the two surfaces are often tightly coupled, effectively with a high fracture stiffness, and the effect of the fractures is primarily evident when failure, such as frictional sliding or tensile opening, has occurred.

The displacement discontinuity model of a fracture has also been studied for seismic wave propagation (Schoenberg, 1980; Myer et al., 1985; Myer et al., 1995). In this case the fracture stiffness has been shown to have a significant effect on wave propagation. The model has been shown to be consistent with experiments of recorded wave propagation through natural fractures in rock (Pyrak-Nolte et al., 1990a), in particular accounting for frequency-dependence of both the wave-speed and the amplitude. Researchers have also developed expressions for transmission and reflection coefficients based on different assumptions about coupling of the surfaces of the displacement discontinuity model.

Accurate modelling of wave propagation in the fracture zone requires that the wave behaviour is accurate for a considerable number of fractures and for the entire duration of oscillation. Consequently, the emphasis in this section is to accurately reproduce full waveforms for experimental data involving multiple fractures. The selected experiments were for wave propagation through a series of stacked steel plates (Pyrak-Nolte et al., 1990b). These experiments extended earlier results on single natural fractures (Pyrak-Nolte et al., 1990a). In the experiment, 31 mild steel plates were sandblasted to simulate fracture surfaces, and bolted to form a cube of side 90 mm. The block was biaxially loaded at 30 kN , one load clamping the plates and a second parallel to the plates. P- and S-wave transmission was recorded for different orientations of the layered block and also for a solid steel cylinder to provide a control.

The experiment was modelled in three dimensions using 0.75 and 5.5 million fourth order accurate finite different zones for the P- and S-wave models respectively. The fractures were modelled using

zero-thickness displacement discontinuities. Source waveforms for the P- and S-wave experiments were inverted from the waveform through the solid steel cylinder using Fourier transforms and applying the formula:

$$I_{Exp}(\omega) = \frac{O_{Exp}(\omega)}{O_{Tst}(\omega)} I_{Tst}(\omega) \qquad (2)$$

where I_{Exp} is the inverted source waveform, O_{Exp} is the observed experimental response for solid steel, I_{Tst} is an arbitrary broad frequency test pulse and O_{Tst} is the response in the model of the solid cylinder to the test pulse. These inverted sources were then applied when modelling the fracture cases.

Three simulations were made for P-wave propagation - the solid cylinder, horizontal fractures with wave propagation across the fractures, and vertical fractures with wave propagation parallel to the fractures. Four simulations were made for S-wave propagation - the solid cylinder, horizontal fractures with wave propagation across the fractures, and two different polarisations for vertical fractures with wave propagation parallel to the fractures. In the first polarisation the excitation is parallel to the fractures (SH), while in the second the excitation is transverse to the fractures (SV). Initial models used a uniform normal and shear fracture stiffness of $6*10^{13}$ Pa/m and $2*10^{13}$ Pa/m respectively, based on analysis from the original experiment.

The modelled and recorded waveforms are compared in Figure 2. In each case, the solid model matches the experiment as expected from the source inversion. Both P- and S- wave propagation across the fractures (Ib and IIb) are significantly delayed, and attenuated, with a lower dominant frequency than the solid cases. Similar effects, with delayed arrival and reduced amplitude and frequency, are observed in the model, but to a much lesser degree than in the experiment. In all cases for propagation parallel to the fractures (Ic, IIc and IId), the modelled waveforms are very similar to the observed waveforms. The effects on arrival and amplitude are not as severe as for wave propagation across the fractures, but the waveforms are significantly altered by the fractures and these changes are accurately predicted by the model. The thesis further compares the different cases in terms of time-domain and frequency effects and the effects on wave propagation patterns.

Overall there is a striking correspondence between the modelled waveforms and the recorded waveforms. This is primarily true for all cases of wave propagation parallel to the fractures. The modelled wave propagation across the fractures show similar effects on the arrival, amplitude and frequency to that observed in the experiment, but the model grossly underestimates the degree of attenuation and arrival delay.

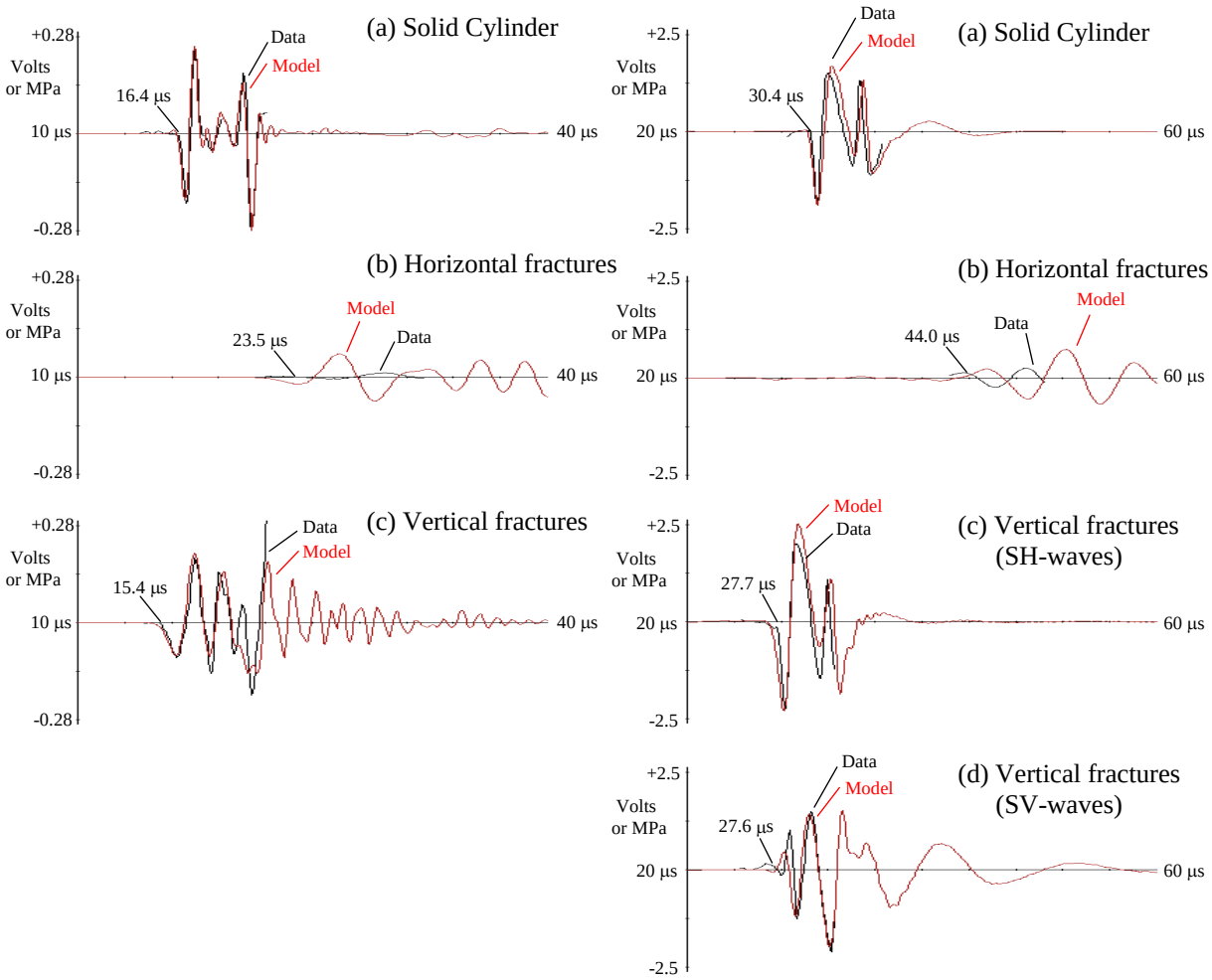

Figure 2 P- and S-wave comparisons of experimental and modelled waveforms for the different fracture orientations.

Variations were made to the fracture stiffness values to determine if improvements could be made for wave propagation across the fractures. Improved estimates of K_n = 4.5*^{13} Pa/m, and K_s = 2.5*10^{13} Pa/m were obtained, but improvements were not significant. It was concluded that the arrivals and amplitudes could not be more consistently matched with a uniform value of fracture stiffness.

The variations also produced a very important result in that the P-wave amplitude is significantly dependent on the crack shear stiffness. This is not predicted by the theory for normal incidence on a single crack. This influence is negligible for small numbers of cracks, but increases rapidly with increasing numbers of cracks, implying that this behaviour is due to multiple reflections.

The discrepancy in waveforms for propagation across the fractures leaves some doubt whether the model captures enough of the physics of the crack, and whether it is suitable for representing wave propagation in the fracture zone. The differences in wave amplitude could indicate an additional dissipative mechanism in the fracture which removes mechanical energy from the system. This would be a fundamental alteration to the displacement discontinuity model. However, it was realised that the loading conditions in the experiment were not uniform. Fracture stiffness is related to the compression of a crack and varies with normal stress across a fracture. A non-uniform stress field implies that rather than a single uniform fracture stiffness, the fracture stiffness should vary for different fractures, and also across an individual fracture. A new model was implemented with a stress-dependent fracture stiffness, based on a hyperbolic joint stiffness relation (Bandis et al., 1983).

Applying the non-uniform loading led to a non-uniform distribution in fracture stiffness, and was shown to give improved matches due to greater attenuation and delay. The reason for the reduction in amplitudes in the stress-dependent model is apparent from the patterns of wave propagation (Figure 3). The uniform fracture stiffness model (3a) has wave-fronts which remain coherent across the whole block. Waves in the stress-dependent fracture stiffness model (3b) propagate faster and more strongly through the centre of the model, leading ultimately to greater scattering of the wave. This indicates that the non-uniform loading leads to a non-uniform distribution in fracture stiffness, and can account for lower amplitudes without introducing a radical change to the displacement discontinuity model.

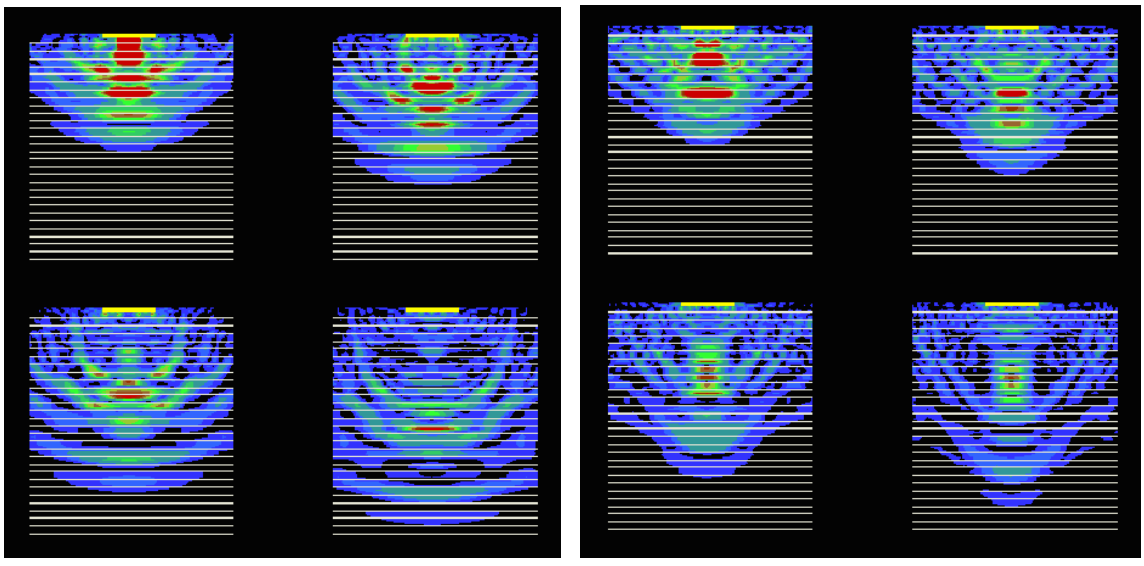

(a) Uniform fracture stiffness (b) Stress-dependent fracture stiffness

Figure 3 Snapshots of particle velocity showing P-wave propagation through the horizontal crack model for (a) uniform stiffness cracks, and (b) stress-dependent stiffness cracks.

This work has shown that modelling wave interaction with displacement discontinuities captures much of the physics observed in experiments. A relatively simple model of a fracture convincingly matched the results of an experiment with many fractures. The work highlights the importance of fracture stiffness for modelling waves through fractures, as it has a significant effect on the waveforms, arrival, amplitude and frequency. Importantly, except in a completely uniform stress field, modelling wave propagation without considering the stress variation, is inaccurate. The stress-dependence of fractures can be accounted for with a stress-dependent fracture stiffness, and in a non-uniform stress field this stiffness may vary along a single continuous fracture. This has important consequences for modelling fractures around underground openings where stresses are highly non-uniform.

4. Models of wave propagation through *in situ* fracturing around an underground excavation - a Case Study from the URL

A number of controlled *in situ* experiments have been made at the Underground Research Laboratory in Canada (URL). This chapter uses ultrasonic velocity scans, collected during an acoustic emission experiment at the URL (Carlson and Young, 1993), to extend the wave-fracture modelling to *in situ* fractures in rock at the surface of a deep tunnel. Their experiment monitored changes in a small volume of rock, approximately one cubic metre, near the face of an advancing tunnel. The velocity scans showed variations in both wave-speed and amplitude for different paths and interpretations were made on the fracturing.

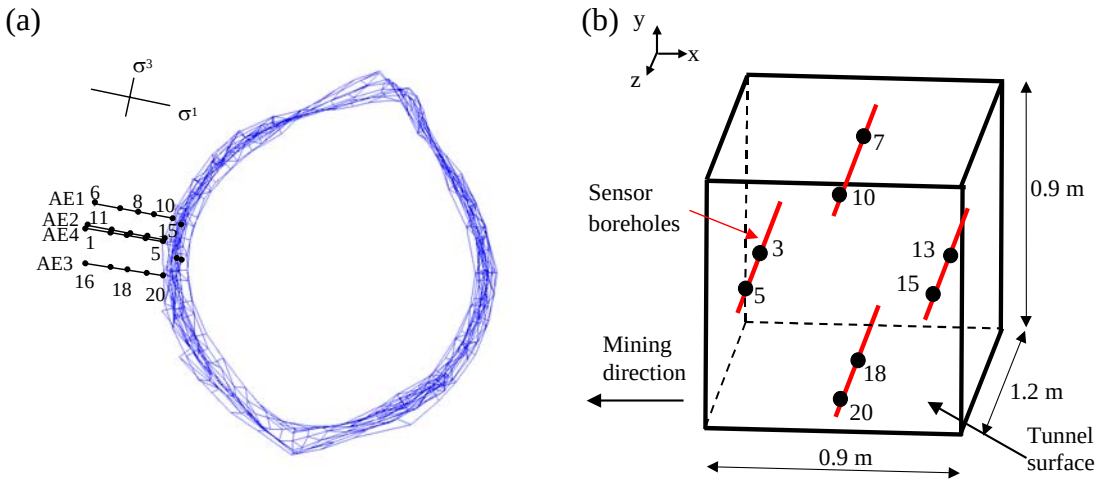

Figure 4 (a) Cross-sectional geometry of the acoustic array in the URL tunnel showing positions of boreholes AE1-AE4, and sensors 1-20. (b) Model geometry of a reduced 8x8 array, with boreholes rotated into a diamond pattern. The block indicates the model boundaries.

The experiment was modelled in three-dimensions (Figure 4), for a reduced 8x8 array of source-receiver combinations, and a model size of around 8 million zones. The tunnel surface was approximated as a flat free-surface. Initial models used an isotropic elastic medium, with the elastic wave-speeds of the intact rock. The ultrasonic sources were modelled by applying a velocity normal to the sensor orientation. Comparisons with the recorded waveforms showed many similarities such as the correct polarities for all P- and S- waves. However, all paths oblique to the tunnel surface were slower and of much lower amplitude than the elastic waveform. The full set of waveform comparisons with the source at sensor 3 are presented in Figure 5.

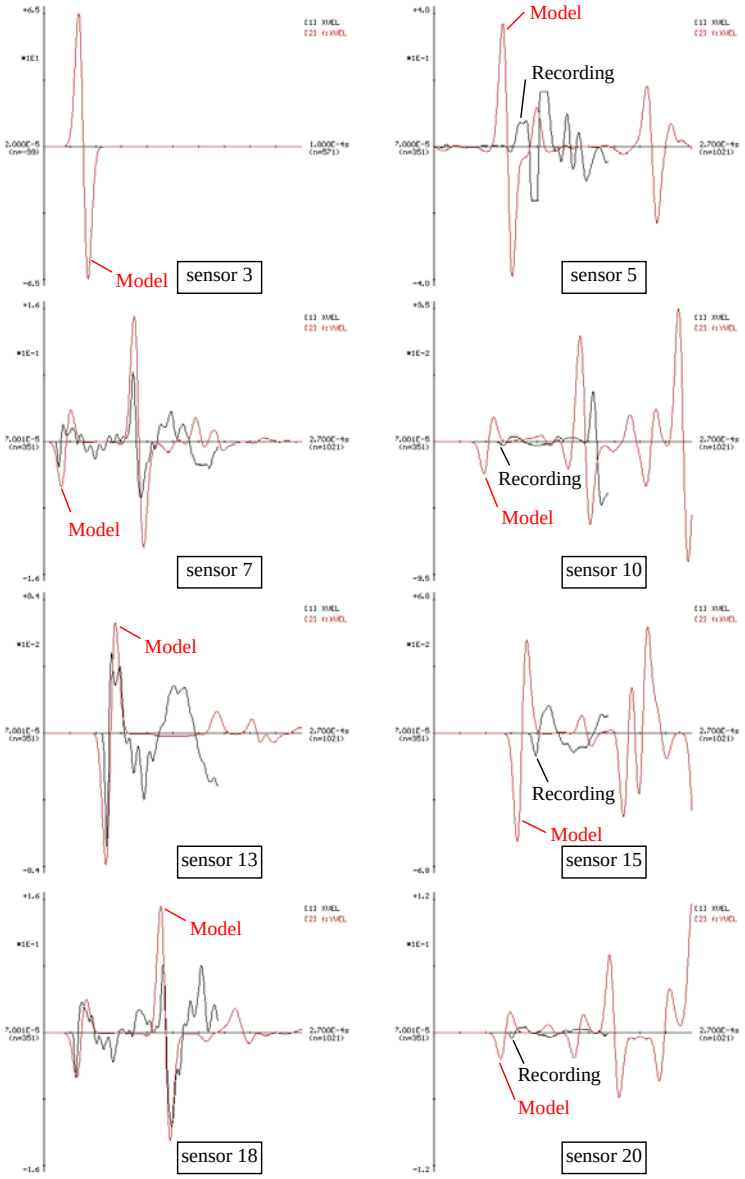

Figure 5 Elastic model (red line) compared to velocity scan AT01 (black line) for the source at sensor 3 – and receiver sensors 3, 5, 7, 10, 13, 15, 18, 20. Paths on the left were parallel to tunnel surface while those on the right were oblique to the tunnel surface.

The elastic model identified that paths parallel to the tunnel surface are approximately elastic, while paths oblique to the tunnel surface are significantly lower than expected in both wave-speed and amplitude. Differences between the two path types were also evidenced in the frequency content of the waveforms. This indicates fractures aligned approximately parallel with the tunnel surface. Carlson and Young (1992) estimated the crack density to range between 0.12 and 0.09. Two methods were used to investigate the fracturing.

One conceptual model of fracturing is a collection of flat openings. A program was written to generate random crack assemblies with a specified crack density and range of crack sizes. Crack density is a dimensionless quantity describing a collection of cracks (O'Connell and Budiansky, 1974). For circular cracks, crack density is proportional to the cube of the crack radius. For rectangular cracks used in WAVE, crack density is given by

$$\varepsilon = \frac{1}{\pi V} \sum \frac{A^2 B^2}{A + B} \tag{3}$$

where A and B are the crack side-lengths, and V the volume of cracked region. A number of numerical issues were encountered with the method and are examined in the thesis. Random crack assemblies of various sizes and crack density were introduced into the model of the experiment to examine their effect on the waveforms. Two examples are shown in Figure 6. A second representation of the fracturing was made by introducing large fractures with a fracture stiffness into the model of the experiment. Although more naturally applied as a model of a single fracture with contacts, this work explored whether it can be used to represent the effects of a collection of openings throughout a volume, rather than in a single plane. For it to be a useful, a relationship needs to be established between it and the underlying physical fracture configuration.

Both methods of representing fracturing caused changes in the wave-speed and amplitude of waveforms, of the order of that observed in the data. The recorded behaviour was more consistent with models of smaller open fractures (26 mm) than with that of larger open fractures (196 mm), although practical numerical limits did not allow smaller cracks to be investigated. The modelling confirms that the only single orientation of fractures consistent with the data for these paths, are fractures approximately parallel to the surface. The modelling also suggests that the crack density was over-estimated in the original analysis. Such modelling could benefit acquisition systems, testing the consistency of conclusions based on the data analysis, in particular conclusions on the density, orientation and size of fracturing.

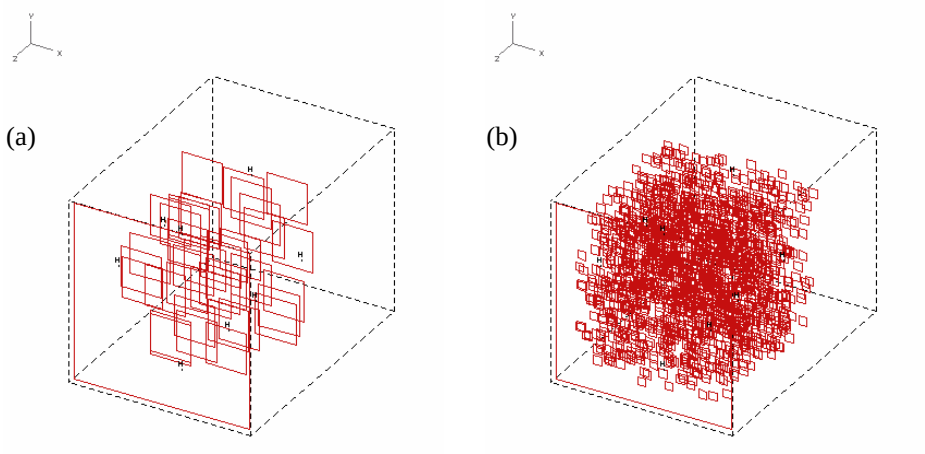

Figure 6 Crack assemblies with equal crack density (ε = 0.1) (a) 38, 196.5 mm x 196.5 mm cracks (b) 6061, 36.5 mm x 36.5 mm cracks.

A qualitative study on the effects of fracture spacing and fracture stiffness indicated that the fracture stiffness had the greatest influence on the amplitude, while decreasing either decreased the wave-speed. In a rough sense, the fracture stiffness may be related to the sizes of openings, while both fracture stiffness and spacing relate to the crack density. The representation using stiff fractures does not suffer from the numerical resolution difficulties associated with the attempts to represent the true size of crack openings, and could therefore be a useful model of effective fracturing for matching the wave behaviour for large scale models. A link then needs to be established between the effective representation and the underlying assembly of fractures.

Motivated by the above, a method was developed to characterize the frequency dependence of both wave-speed and amplitude in fracture models. This was used to understand the effects of crack density and crack size. It explains why models of the experiment with different crack sizes but equal crack densities had different effects on arrival time and amplitude. It also provides a method by which a relationship can be established between models with larger stiff fractures and accumulations of smaller open cracks. A large body of research has focussed on these issues including analytical, experimental and more recently numerical studies. These include developing analytical expressions for wave-speed and attenuation due to fracture assemblies, studying wave propagation through single and multiple aligned stiff fractures, and the relationship of fracture stiffness to areas of contact and opening. The numerical approach used here offers certain benefits over these studies. Expressions are obtained for both attenuation and phase velocity, and these are presented as a function of frequency. The expressions are not limited to wavelengths much larger than the fracture sizes. The analysis is not

necessarily limited to the study of plane waves. Finally, most of the cases necessarily require a three-dimensional treatment, which has not been attempted in other numerical studies.

The method is based on developments in Chapter 2, approximating plane wave propagation through a model with fractures. A recording (waveform-2) is made at the end of the fractured region and compared against the waveform from a perfectly elastic medium recorded at the start position of the fractured region (waveform-1). Using Fourier Transforms of the waveforms, phase velocity (*c*) and attenuation (*A*) can be calculated as a function of frequency *(ω)* from

$$c(\omega) = \omega \left| x_2 - x_1 \right| \left[\frac{-(\phi_2 - \phi_1) - iLn\left(\frac{A_2}{A_1}\right)}{(\phi_2 - \phi_1)^2 + \left[Ln\left(\frac{A_2}{A_1}\right) \right]^2} \right] \tag{4}$$

$$A(\omega) = \left(\frac{A_2}{A_1}\right)^{\frac{L}{|x_2 - x_1|}} \tag{5}$$

where $A_1(\omega)$ and $A_2(\omega)$ are the Fourier amplitude functions and $\phi_1(\omega)$ and $\phi_2(\omega)$ the Fourier phase functions of the elastic and recorded waveforms respectively, x_1 and x_2 are the positions of the recorded waveforms and L is the unit distance of interest. (It is also possible to calculate Q(ω) from the attenuation function and the phase velocity).

The procedure is demonstrated in Figure 7 with results shown in Figure 8a. Significantly, the time domain waveforms do not necessarily show a clear difference in arrival time (Figure 7b). This is due to the high frequencies contained in the source, which are attenuated but not slowed for this crack-size. In contrast, the phase difference (Figure 7c) and the calculated phase velocity (Figure 8a) clearly indicate a reduction in velocity for the low frequency region. The results for phase velocity calculations were found to be consistent and repeatable, but sensitive to certain numerical issues, primarily related to practical limits on the model size. The models were then at the limit of capability with approximately 12 million grid-points.

A wide range of fracture sets were studied using this method, including random distributions of a large number of small open cracks of varying size and crack density, and larger fractures with surfaces coupled by a fracture stiffness. Some typical results are shown in Figure 8. The curves indicate that wave-speed is not constant with frequency. It decreases from its low frequency value by another

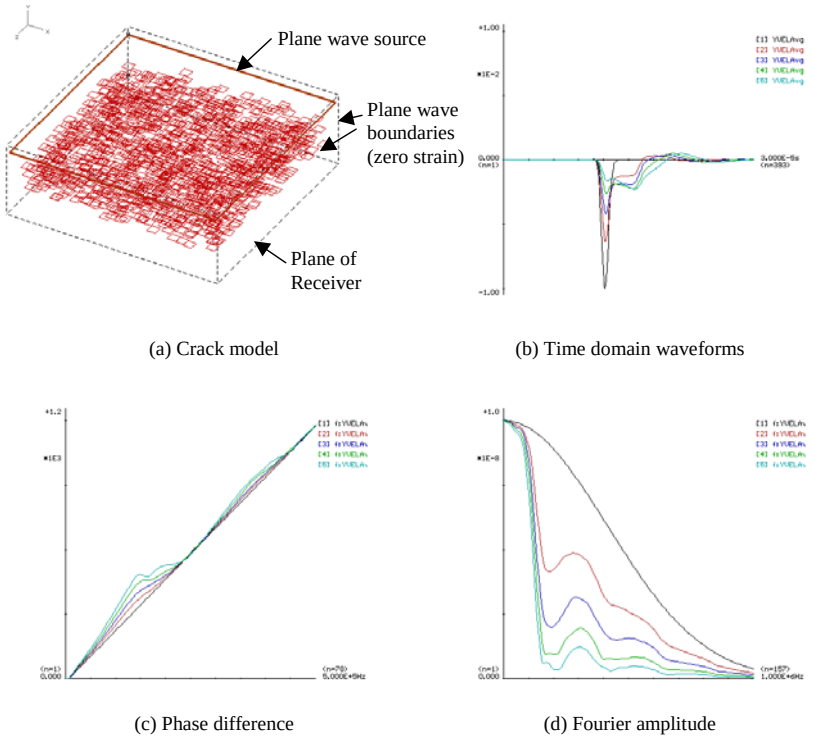

(a) Crack model (b) Time domain waveforms

(c) Phase difference (d) Fourier amplitude

Figure 7 Stages for calculating phase velocity and attenuation (a) Simulated fracture medium (b) Time domain waveforms for the crack models (c) Phase spectrum difference between emerging and input waveforms (d) Fourier amplitude spectrum. Models have 11.3 mm cracks with 296, 591, 887 and 1182 cracks respectively, corresponding to crack densities of 0.025 (red), 0.050 (blue), 0.075 (green) and 0.1 (cyan), and are compared to an uncracked model (black). The resulting phase velocity and attenuation functions are shown in Figure 8a.

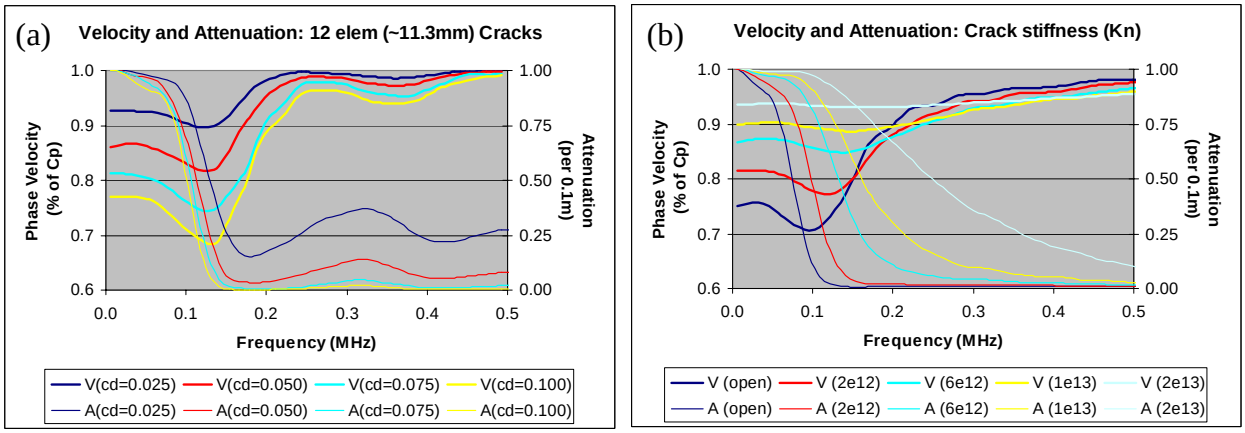

Figure 8 Phase velocity and attenuation spectra for crack distributions. (a) Distribution of 11.3 mm open cracks with a crack density of 0.025, 0.05, 0.075 and 0.1. (b) Distribution with crack lengths ranging from 7.3 mm to 19.3 mm, a crack density of 0.1, and varying fracture stiffness.

30-50%, and then increases back toward the elastic wave-speed such that high frequencies are attenuated but not slowed. Increasing crack density leads to successive decreases in the low frequency phase-velocity. Studies also showed that an increase in fracture stiffness increases the phase velocity and shifts the frequency at which high attenuation occurs to a higher frequency, a change consistent with that of a lower crack density and smaller open cracks. The work has important implications for seismic interpretation in that wave-speeds measured in the time-domain cannot be used to uniquely determine crack density. Overall a useful quantitative approach has been developed for numerically investigating the effects of fractures.

5. Evaluating the influence of an excavation on the distribution and amplitudes of ground motion

The previous chapters developed models which indicate success in duplicating the behaviour of measured wave propagation through fractures. There are two potential applications. The potential to aid the interpretation of fracturing around excavations, has been demonstrated. The second application is to improve the forward modelling of wave propagation around underground openings. This chapter returns to the rockburst problem discussed in the introduction, and considers the effect of the excavation and fracturing on the ground motions in excavations.

Understanding the maximum ground motions due to a rockburst, its decay, and the regions of large ground motion, has important consequences for hazard analysis and support design. However, a number of questions remain unanswered in the field of rockburst study. What are the maximum in-stope amplitudes caused by a seismic event (McGarr, 1993; Ortlepp, 1993; Spottiswoode et al., 1997)? What mechanisms lead to motions in stopes being much larger than those in the solid rock (Hemp and Goldbach, 1993; Milev et al., 1999)? What affects the observed distribution of damage and why does damage sometimes occur at large distances from the original event (Durrheim et al., 1997)? This section uses models to evaluate the effect of the excavation on ground velocity and in so doing attempts to address these questions. It first evaluates the influence of the stope's free surface alone and highlights certain features of Rayleigh waves. It then examines the effect of variations in the geometry and source on the amplitude of ground motion. Different representations of the fracture zone are introduced to determine whether this indeed leads to amplification. Finally, it considers the potential for triggered energy release to cause increased ground motions.

A mining problem is used throughout this section to examine the effects of an excavation on wave propagation. It consists of a tabular stoping geometry typical of long-wall mining in deep-level mines in South Africa. Figure 9a shows a plan view of the mining layout with the mining direction towards

the right. The mining layout consists of the stope, which is a narrow excavation of 1.5 metres height extending for hundreds of metres, and pillars, which are solid regions left for stability reasons. The 'stepped' outline shows the mining face position or lead-lag face. The pillars are highly stressed and hence can be the source of seismicity. Wave propagation was simulated for a vertical slip event in the foot-wall of the pillar. The region of slip was 28 m by 28 m, with source centre 2 m into the pillar, 12 m below the stope, and 12 m back from the stope face (Figure 9a). The rupture was propagated at 3000 m/s, with a uniform stress drop of 9.35 MPa. The stress drop at any point occurred over 2 ms, and the whole event over 6 ms. The event had a moment of $1.2*10^5$ MNm, and a moment magnitude of 1.3.

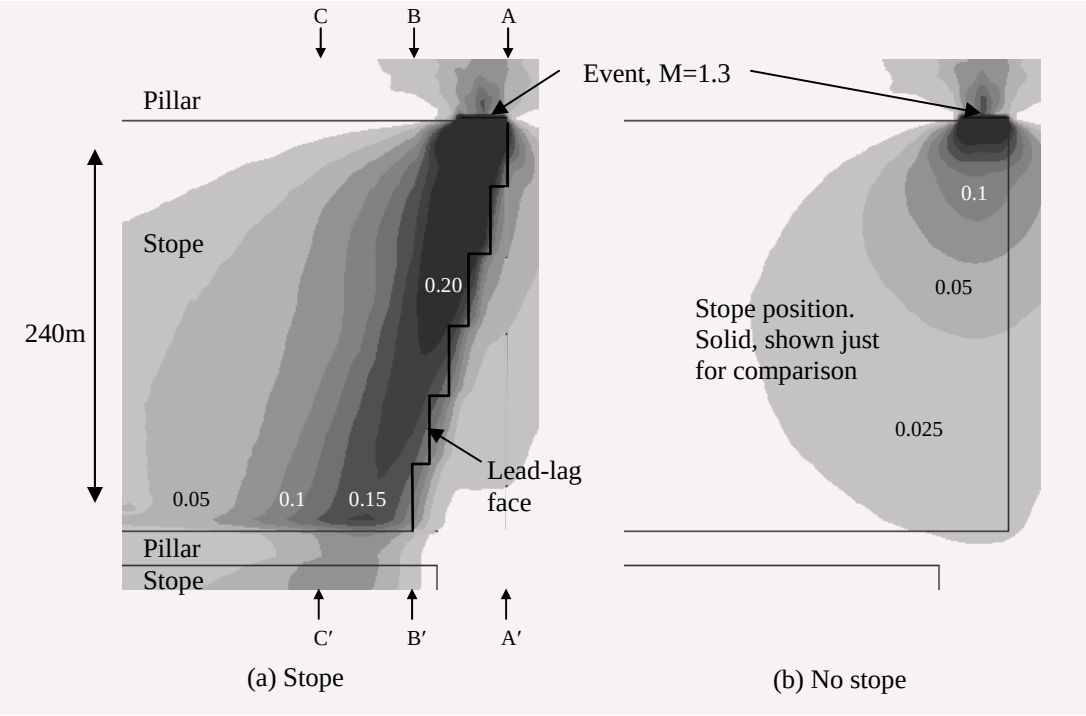

Figure 9 The projected influence of a mining layout on the wave propagation from a seismic event. Plan sections are shown through two three-dimensional elastic models. One contains a tabular mining excavation, the other a purely solid material. Contours indicate the maximum vertical velocity (m/s), induced by a particular seismic event of magnitude 1.3, in a plane just below the excavation. The event occurred in the foot-wall of the pillar, parallel to the direction of mining advance, just behind the face position of the mining. The influence of the stope on the wave propagation causes velocities at a far pillar to be up to six times that of the solid model without the excavation.

Figure 9 compares the maximum vertical velocity in a plane 2 m below the stope with the case if the excavation did not exist. The excavation significantly influences both the amplitude and the distribution of the largest motions. Maximum amplitudes follow the face outline, and the maximum amplitudes deep into the stope are around four times those at similar distances in the solid model. An

even more marked effect is observed in the induced tensile stresses, where the value 200m from the event is increased from 0.06 MPa in the solid model to 1.6 MPa due to the influence of the excavation. Figure 10 indicates that the distribution of tensile stress at the surface is very similar to that of the maximum velocity, but decays sharply with distance from the free surface. It is hypothesised that this induced stress may be significant in triggering energy release in the low stress failed regions of the stope hanging-wall and foot-wall, or in the highly stressed regions of the pillars.

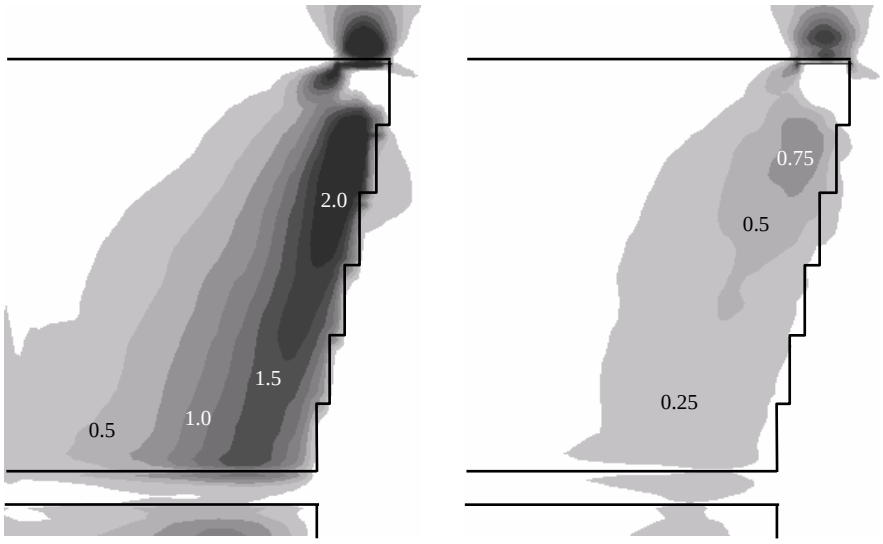

(a) 2m below stope (b) 6m below stope

Figure 10 Maximum induced tensile stress (in MPa) for σ_{zz}. Plan sections are shown for two distances below the excavation, and indicate that horizontal tensile stress of up to 2 MPa is induced close to the surface, and that this falls off rapidly with distance from the surface.

It is significant that just a 1.3 magnitude event near the edge of a stope can lead to these motions and induced tension 200 m from the event. This is caused by surface waves propagating along the free surface of the stope, although for these wavelengths and distances the shear and Rayleigh waves do not separate, and motion is made up of both body and surface waves. A study was made of Rayleigh waves propagating along the hanging-wall of an infinite stope. Figure 11 compares the decay in velocity and tensile stress for two different sources with peak frequencies of 330 Hz and 120 Hz. For small, high frequency events, the decay is rapid, and velocity at the surface is many times more than that a few metres into the solid. Measurements have been made where particle velocities were many times higher at the surface than a few metres into the fracture zone (e.g. Milev et al., 1999), and this has been interpreted as amplification due to the fracture zone. The above analysis shows that some of the apparent amplification may be explained by Rayleigh waves rather than by the effect of the fracture zone.

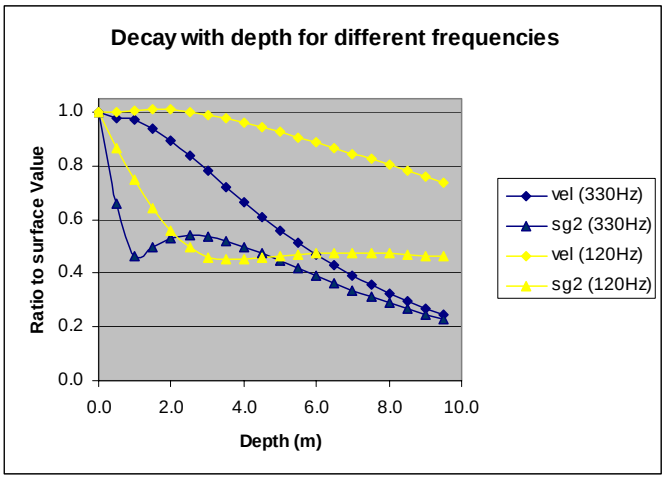

Figure 11 Decay rate of velocity and maximum tensile stress for different frequencies. (a) Peak frequency of 330 Hz ($\lambda \approx 10$ m) (b) Peak frequency of 120 Hz ($\lambda \approx 27$ m)

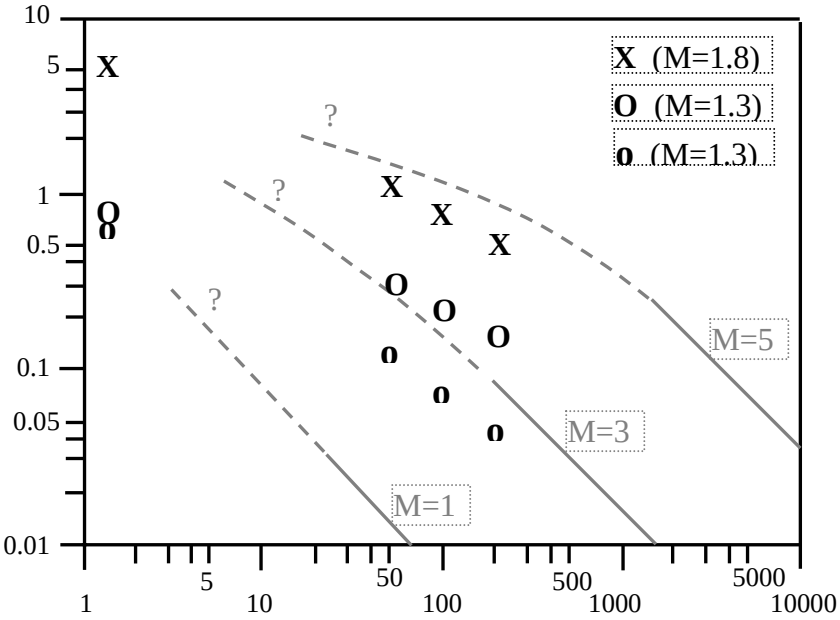

Figure 12 Far-field and projected near-field velocities for different magnitude events (from Jager and Ryder, 1999). Velocities for three of the modelled events have been superimposed on the original graph. The presence of the stope, and cases with a high stress-drop, lead to in-stope velocities associated with much larger magnitude events.

The layout of Figure 9 was further analysed to determine the effect of variations in the source, such as higher stress-drops, orientation of slip and proximity of source to stope (including intersection with the stope, termed 'daylighting'), on peak velocities. The peak near-source velocities were up to 70%

higher than upper limits commonly estimated using the formula ($V_{max} \approx 1.1\tau_e/(G\beta)$), (Jager and Ryder, 1999). Figure 12 shows a graph from Jager and Ryder (1999) of far-field velocities and estimates of near-field velocities for different magnitude events, with values from three of the modelled events superimposed. The two modelled events which include the excavation, have much higher velocities, and decay more slowly than that projected by Jager and Ryder. The presence of the stope therefore leads to in-stope velocities normally associated with much larger magnitude events.

The hanging-wall and foot-wall of deep-level mining stopes are highly fractured due to stress-induced fracturing and natural discontinuities. Fractures cause waves to attenuate due to scattering of high frequencies, but also reduce the effective elastic modulus of rock, which may increase amplitudes for long wavelengths. The effect of fractures on the peak near-field and far-field velocities was therefore evaluated for stope-normal (vertical) and stope-parallel (horizontal) fractures. Figure 13 shows two cases for vertical fracturing with crack densities of 0.01 and 0.1. Vertical fractures had no effect on the near-field amplitudes, but horizontal fracturing increased the peak near-field velocities (by up to 50% for some models). Both orientations of fractures accounted for increased amplitudes at more distant parts of a stope. The amplitudes decrease if the fracture stiffness is low, which may indicate that the propagation of surface waves is inhibited by very open fractures. The fracturing also affects the distribution of maximum velocity and the waveforms.

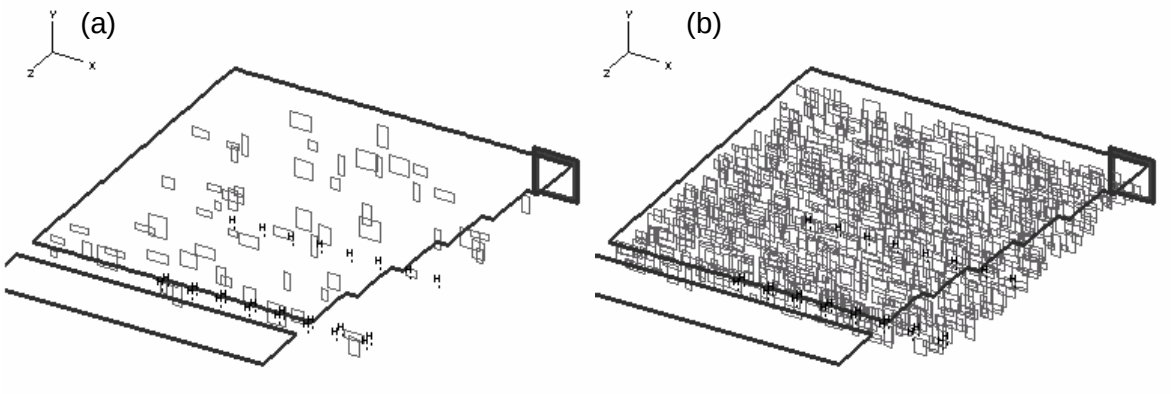

Figure 13 Stope model with vertical fractures in the foot-wall of the stope. The fractures are rectangular with edge-lengths between 4 m and 14 m, and are in a band between 4 m and 18 m below the stope. (a) Fracture density of 0.01 (b) Fracture density of 0.1

Although the models showed that even small magnitude events can account for maximum velocities of more than 1 m/s, much larger velocities have been inferred in observations of failed rock (Ortlepp, 1993). One explanation for large velocities is that the waves may trigger failure in a highly stressed

region (e.g. within a buckling slab, McGarr 1997). Another model proposed by Linkov and Durrheim (1998), is amplification due to additional energy release as waves pass through the fracture zone which is in a post-failure, strain-softening state. A related mechanism was investigated by assuming residual stresses on the fractures and investigating whether waves from the event would cause additional energy release and whether this would increase the amplitude of the wave motions. The results were that some failure took place on all fractures, generating source magnitudes on individual fractures ranging from -2.5 to 0.35, and a total moment of 6.10^5 MNm - five times that of the original event. Nevertheless, the distribution of maximum velocity was no larger than the original event, and motions were smaller than that obtained with soft, linear fractures. There were, however, pockets of high velocity associated with triggered events in areas where there was previously low ground motion, and seismograms were also considerably altered. The conclusion is that although considerable energy release occurs, this is not coherent and does not lead to the amplification of the original wave, but rather manifests itself in localised pockets of large motions, sometimes in unexpected areas.

This work has shown that the amplitudes in both the near- and far- field are complexly influenced by the following: stress drop, sense of slip, excavation surface, excavation outline, and the proximity of any part of the source, rather than the source centre, to the excavation. In these models, the stope free-surface caused up to a 40% increase in near-field and up to a 600% increase in far-field velocities, while fracturing caused up to a 50% increase for both near- and far-field stope velocities. The conclusion is that the damage potential from an event near an excavation cannot be readily inferred from aspects such as moment, magnitude and the proximity to the source centre, as this ignores the effect of free surfaces and fracturing.

6. Conclusions and Practical Implications

This thesis contributes to science and technology through an improved understanding of wave propagation through fractured rock and the increased ability to model such behaviour. It has capacity for real world application in many engineering fields such as mining, underground waste depositories and oil exploitation. This chapter presents conclusions on fracturing, real world applications and numerical issues.

(i) Representation of fracturing

Repeated use of two simple models of a fracture, was successful in reproducing experimental recordings of wave propagation through a large number of fractures.

- Complex three-dimensional wave behaviour has been realistically modelled using a mechanistic model of fracture, specifically a displacement discontinuity. Although based on theoretical

models developed some years ago, this is possibly the first numerical demonstration that a mechanistic model of fracturing can accurately reproduce significant changes in waveforms in non- plane-wave propagation through multiple fractures.

- The fracture stiffness significantly affects the waveforms, delay, amplitude and frequency content, and the degree of attenuation of high frequencies and amplification of lower frequencies.
- The shear fracture stiffness influences the amplitude of first arrivals, for P-wave transmission through multiple fractures. This is an important result, which is not predicted by the theory for a single fracture.
- The importance of stress-dependence on the fracture stiffness was established. A model with stress-dependent fracture stiffness was investigated and the stress state significantly affected wave propagation. It is not sufficient to simply allow opening of fractures in tension, as significant differences in wave propagation occur even when all fractures are in compression.
- Two explicit models of fracturing were used - fractures with a fracture stiffness and accumulations of small open cracks. Both accounted for observed effects on wave-speed and amplitude, for waves across fractures and for waves parallel to fractures.
- It is presently impractical to model the true openings in the material to account for waveform changes in *in situ* monitoring. The wave propagation changes on a larger-scale can be more readily accounted for by using a distribution of stiff rather than open fractures. Some applications require understanding the underlying openings, for example for fluid flow. Smaller-scale wave models would then be used to investigate how the effective fractures relate to an underlying physical state.
- A numerical technique was developed to characterise the wave behaviour for various models of fracturing and across a wide frequency band. The technique has advantages over theoretical analyses, allowing less restrictive cases to be studied and can be readily applied to alternative models of fracture. The method involves simulating plane wave propagation through an assembly of fractures and extracting the frequency variation in phase velocity and attenuation from the resulting waveforms.
- Phase velocity and attenuation spectra were calculated for various sizes and densities of open fractures, as well as for large fractures with varying fracture stiffness and fracture spacing. The technique can readily be applied to study a much wider range of fracture models and has the capacity to provide greater insight to interpretations of fracturing from seismic recordings.

(ii) Capacity for real world application

Two main applications have been pursued in this work. The first is forward-modelling to project the wave propagation around underground openings. Reliable models of wave propagation can have important benefits for hazard analysis, since understanding the amplitude and distribution of ground motions is the first step in anticipating regions of likely damage due to seismic events. This goal has

been advanced by modelling case studies where the wave behaviour was shown to correspond to observed behaviour, albeit in highly-controlled experimental conditions.

The second application is to aid the analysis of recorded data to interpret the fractured state of rock. This is important to the fields of mining, oil extraction and nuclear waste storage. Models allow the interpretation to go beyond average seismic properties of rock (wave-speeds and attenuation) and to help interpret the underlying structure of fracturing and stress-state, giving a physical basis for the wave-speeds and attenuation derived by seismic analysis. Models also allow conclusions on the density, orientation, size of fractures, and the stress state, to be verified. The potential for this has been established through the modelling of the URL data, where insight was given into the crack density and the size of open cracks.

A number of specific conclusions are important for the modelling of waves around openings:

- The results on fracture stiffness have important consequences for modelling waves around underground openings. Large fractures should not be considered as simply open or closed.
- The stress distribution around underground excavations is extremely non-uniform and the stress-dependence of the fracture stiffness is important for modelling wave propagation around these openings.
- The dependence of fracturing on stress state indicates that projecting the wave propagation around openings is ultimately a coupled problem of solving the *in situ* stress state together with the seismic loading.
- The study indicates that coupling modelling with the measurement of seismic waveforms will aid in interpreting the rock mass condition. The modelled fracturing causes both wave-speed and amplitude changes and provides a method of verifying the consistency of conclusions acquired through seismic monitoring.
- It was found to be presently impractical to model the true crack openings in the material for *in situ* monitoring. A two-phase approach was proposed, where the true openings can be investigated in smaller-scale models.
- The approaches used for modelling the ultrasonic source and for inverting for the source are useful for future analysis of such data.
- Amplitudes of ground motion in both the near- and far- field are complexly influenced by stress drop, sense of slip, excavation surface, excavation outline, and the proximity of any part of the source, rather than the source centre, to the excavation. Fractures influenced amplitudes in both the near-source and far-field region.
- A number of different causes were identified as possible explanations for the apparent amplification reported by researchers in this field.

- The damage potential from an event near an excavation cannot be simply inferred from aspects such as moment, magnitude and the proximity to the source centre, as this ignores the effect of the excavation and fracturing.

Numerical contributions

A number of numerical contributions have been made which are important for models of wave propagation around underground openings:

- It was shown that a finite difference approach could be used to study wave interaction with a very large numbers of fractures.
- A coupled solution including static loading is important to obtain the correct behaviour of waves though fractures and an efficient method was proposed for a larger graded static mesh which does not affect the resolution and efficiency of the dynamic model.
- A numerical method was developed which allows the dispersion characteristics of a numerical code to be studied. The approach calculates the variation of phase or group velocity and amplitude with frequency, without any need to analyse the underlying method. This allowed the accuracy and efficiency of a number of codes to be examined and results support the need for specialised codes for studying wave propagation.
- A number of methods were investigated for generalising the staggered grid scheme to support angled cracks. A scheme based on a localised transversely isotropic material was found to be unsuitable. A second order approximation to an explicit angled crack was developed, although the method is not suited for modelling completely general fracture geometries. A scheme was derived for mapping the orthogonal grid to a curvilinear grid but the implementation of a crack requires derivatives which are not readily approximated in the staggered mesh.
- A new finite difference scheme was developed which is 4^{th} order accurate in space, does not exhibit hour-glassing, and has a memory and run-time efficiency comparable to that of the staggered mesh. The different components of stress are held at the same point in space, giving it an advantage over the staggered mesh for more general studies of fracturing, cavities or free surfaces.

References

Aki K. and Richards P.G. (1980), *Quantitative Seismology: Theory and Methods*. Freeman, Cooper, San Francisco, Vol. 2, section 13.6, pp. 773-795.

Bandis, S.C., Lumsden, A.C., and Barton, N.R. (1983), Fundamentals of rock joint deformation. Int. J. of Rock Mech., Vol. 20 (6), pp. 249-268.

Carlson, S.R. and Young, R.P. (1992), Acoustic emission and ultrasonic velocity study of excavation-induced microcrack damage in the mine-by tunnel at the underground research laboratory. Report #RP015AECL to Atomic Energy of Canada, pp. 1-50.

Carlson, S.R. and Young, R.P. (1993), Acoustic emission and ultrasonic velocity study of excavation-induced microcrack damage at the underground research laboratory. Int. J. of Rock Mech., Vol. 30 (7), pp. 901-907.

Coates, R.T. and Schoenberg, M. (1995), Finite-difference modelling of faults and fractures. Geophysics, Vol. 60 (5), pp. 1514-1526.

Cook, N.G.W. (1992), Natural joints in rock: Mechanical, hydraulic and seismic behaviour and properties under normal stress, Internat. J. Rock Mech, Min Sci. Geomech Abstr, Vol 29, pp. 198-223.

Crampin, S. (1981), A review of wave motion in anisotropic and cracked elastic-media. Wave Motion, Vol. 3, pp. 343-391.

Cundall, P.A. (1992), Theoretical basis of the program WAVE. Unpublished internal report, COMRO (now CSIR Division of Mining Technology, South Africa), pp. 1-12.

Durrheim, R.J., Roberts, M.K.C., Hagan, T.O., Jager, A.J., Handley, M.F., Spottiswoode, S.M., and Ortlepp, W.D. (1997), Factors influencing the severity of rockburst damage in Southern African gold mines. Proc. of 1st Southern African Rock Engineering Symposium (SARES), Johannesburg, South Africa, pp. 17-24.

Graves, R.W. (1996), Simulating seismic wave propagation in 3D elastic media using staggered-grid finite differences. Bulletin of the Seismological Society of America Vol. 86 (4), pp. 1091-1106.

Hemp, D.A., and Goldbach, O.D. (1993), The effect of backfill on ground motion in a stope. Proc. 3rd Int. Symp. on Rockbursts and Seismicity in Mines, ed. Young, Balkema, pp. 75-79.

Hestholm, S. and Ruud, B. (1994), 2D finite-difference elastic-wave modeling including surface-topography. Geophysical Prospecting, Vol. 42 (5), pp. 371-390.

Hildyard, M.W., Daehnke, A., and Cundall, P.A. (1995), WAVE: A computer program for investigating elastodynamic issues in mining. Proc. 35th U.S. Symp. on Rock Mech., June 1995, Balkema, pp. 519-524.

Hildyard, M.W. (1995), WAVE Developments. In *Develop a quantitative understanding of rockmass behaviour near excavations in deep mines*. Unpublished SIMRAC final project report (GAP029), December 1995, CSIR Mining Technology, Johannesburg, South Africa, pp.17-51.

Hudson, J.A. (1981), Wave speeds and attenuation of elastic waves in material containing cracks. Geophysical Journal R. Astr. Soc., Vol. 64, pp. 133-150.

Itasca Consulting Group, (1993a), UDEC Version 2.0, Minneapolis, Minnesota.

Itasca Consulting Group, (1993b), FLAC Version 3.2, Minneapolis, Minnesota, pp.1-20.

Jager, A.J. and Ryder, J.A. (1999), *A handbook on rock engineering practice for tabular hard rock mines*. Published by The Safety in Mines Research Advisory Committee (SIMRAC), Johannesburg, South Africa.

Jiangfeng, Z. (1997), Quadrangle-grid velocity-stress finite-difference method for elastic wave propagation simulation. Geophysics J. Int., Vol. 131, pp.127-134.

Linkov, A.M. and Durrheim, R.J. (1998), Velocity amplification considered as a phenomenon of elastic energy release due to softening. Mechanics of Jointed and Faulted Rock, Balkema, pp. 243-248.

Liu, E.R., Hudson, J.A., and Pointer, T. (2000), Equivalent medium representation of fractured rock. J. Geophys. Res., Vol. 105 (B2), pp. 2981-3000.

Madariaga, R. (1976), Dynamics of an expanding circular fault. Bulletin of the Seismological Society of America, Vol. 66 (3), pp. 639-666.

Marti, J. and Cundall, P.A. (1982), Mixed discretization procedure for accurate modelling of plastic collapse. Int. J. for Num. and Analytical Methods in Geomechanics, Vol. 6, pp. 129-139.

McGarr, A. (1993), Keynote address: Factors influencing the strong ground motion from mining-induced tremors. Proc. 3rd Int. Symp. on Rockbursts and Seismicity in Mines, ed. Young, Balkema, pp. 3-12.

McGarr, A. (1997), A mechanism for high wall-rock velocities in rockbursts, Pure and Applied Geophysics, Vol. 150, pp. 381-391.

Milev, A.M., Spottiswoode, S.M., and Stewart, R.D. (1999), Dynamic response of the rock surrounding deep level mining excavations. Proc.9th ISRM Int. Congress on Rock Mech., Paris, pp. 1109-1114.

Molenkamp, F., Kidger, D.J., and Smith, I.M. (1992), Accuracy of four-node standard finite element. Int. J. for Num. and Analytical Methods in Geomechanics, Vol. 16, pp. 323-333.

Myer, L.R., Hopkins, D., and Cook, N.G.W. (1985), Effect of contact area of an interface on acoustic wave transmission characteristics. Proc. 26th U.S. Symp. on Rock Mech., Balkema, pp. 565-572.

Myer, L.R., Hopkins, D., Peterson, J.E., and Cook, N.G.W. (1995), Seismic wave propagation across multiple fractures. In *Fractured and Jointed Rock Masses*, eds. L.R. Myer, N.G.W. Cook, R.E. Goodman and P. Tsang, Balkema, pp. 105-109.

O'Connell, R.J. and Budiansky, B. (1974), Seismic velocities in dry and saturated cracked solids. J. Geophys. Res., Vol. 79, pp. 5412-5426.

Ortlepp, W.D. (1993), High ground displacement velocities associated with rockburst damage. Proc. 3rd Int. Symp. on Rockbursts and Seismicity in Mines, ed. Young, Balkema, pp. 101-106.

Pyrak-Nolte, L.J., Myer, L.R., and Cook, N.G.W. (1990a), Transmission of seismic waves across single natural fractures. J. Geophys. Res., Vol. 95 (B6), pp. 8617-8638.

Pyrak-Nolte, L.J., Myer, L.R., and Cook, N.G.W. (1990b), Anisotropy in seismic velocities and amplitudes from multiple parallel fractures. J. Geophys. Res., Vol. 95 (B7), pp. 11345-11358.

Rockfield Software Ltd., (1999), ELFEN user manual v.2.8, University College of Swansea.

Sayers, C.M. and Kachanov, M. (1991), A simple technique for finding effective elastic-constants of cracked solids for arbitrary crack orientation statistics. Int. J. Solids Structures, Vol. 27 (6), pp. 671-680.

Schoenberg, M. (1980), Elastic wave behaviour across linear slip interfaces. J. Acoust. Soc. Am., Vol. 68 (5), pp. 1516-1521.

Spottiswoode, S.M., Durrheim, R.J., Vakalisa, B., and Milev, A.M. (1997), Influence of fracturing and support on the site response in deep tabular stopes. Proc. of 1st Southern African Rock Engineering Symposium (SARES), Johannesburg, South Africa, pp. 62-67.

Virieux, J. (1984), SH-wave propagation in heterogeneous media: velocity-stress finite-difference method. Geophysics, Vol. 49 (4), pp. 1933-1957.

List of Publications

Hildyard, M.W. and Young, R.P. (2002), Modelling wave propagation around underground openings in fractured rock. Special issue on induced seismicity, ed. Trifu, Pure and Applied Geophysics, Vol. 159, pp. 247-276.

Hildyard, M.W. and Young, R.P. (2002), Modelling wave propagation through multiple rock fractures. 5th ISRM International Workshop on the Application of Geophysics to Rock Engineering, Ed. Young, R.P. and Pyrak-Nolte, L.J.

Hildyard, M.W. and Milev, A.M. (2001a), Simulated rockburst experiment: Development of a numerical model for seismic wave propagation from the blast, and forward analysis. J. South African Inst. Min. Metall., Vol. 101 (5), pp. 235-245.

Hildyard, M.W. and Milev, A.M. (2001b), Simulated rockburst experiment: Numerical back-analysis of seismic wave interaction with the tunnel. J. South African Inst. Min. Metall., Vol. 101 (5), pp. 223-234.

Hildyard, M.W., Napier, J.A.L., and Young, R.P., (2001), The influence of an excavation on ground motion, Proc. 5th Symp. on Rockbursts and Seismicity in Mines (RaSiM 5), Johannesburg, Sept. 2001, S.A. Inst. Min. Metall., pp. 443-452.

Daehnke, A. and Hildyard, M.W. (1997), Dynamic fracture propagation due to stress waves interacting with stopes. Proc. of 1st Southern African Rock Engineering Symposium (SARES), Johannesburg, South Africa, pp. 97-108.

Napier, J.A.L., Daehnke, A., Dede, T., Hildyard, M.W., Kuijpers, J.S., Malan, D.F., Sellers, E.J., Turner, P.A. (1997), Quantification of stope fracture zone behaviour in deep level gold mines. J. South African Inst. Min. Metall., Vol. 97 (3), pp.119-134.

Handley, M.F., Hildyard, M.W., and Spottiswoode, S.M. (1996), The influence of deep mine stopes on seismic waves. Proceedings of the 2nd North American Rock Mechanics Symposium (NARMS), Montreal, pp. 499-506.

Hildyard, M.W., Daehnke, A., and Cundall, P.A. (1995), WAVE: A computer program for investigating elastodynamic issues in mining. Proc. 35th U.S. Symp. on Rock Mech., June 1995, Balkema, pp. 519-524.

Siebrits, E., Hildyard, M.W., and Hemp, D.A. (1993), Stability of backfilled stopes under dynamic excitation. Proc. 3rd Int. Symp. on Rockbursts and Seismicity in Mines, ed. Young, Balkema, pp. 117-121.

Napier, J.A.L. and Hildyard, M.W. (1992), Simulation of fracture growth around openings in highly stressed brittle rock. J. South African Inst. Min. Metall., Vol. 6, pp. 159-168.

Hildyard, M.W. (1989), Design of a disk-based file server involving the mapping of 'psuedo-disks'. *MSc Dissertation*, University of the Witwatersrand, Johannesburg, South Africa.

Hildyard, M.W. (1985), The design and prototyping of a communications computer based on the Intel 80286. *BSc (Elec. Eng.) Dissertation*, University of the Witwatersrand, Johannesburg, South Africa.